

Flexible Antenna Array for Early Breast Cancer Detection using Radiometric Technique

A. Afyf, L. Bellarbi, F. Riouch, A. Errachid, and M. A.Sennouni

Abstract— Radiometry (or Microwave Thermography) as an early non-invasive and highly sensitive method helps on the detection of the malign tumors in the early curable stages, contributing to diminish the mortality which appears in the cases where the breast cancer was detected in late incurable stages. In this paper we present a novel design of an antenna array structure which is a crucial part in a radiometer system. The flexible compact antenna array is composed of two elements coupled with a T-junction, fed by a coplanar waveguide (CPW). Using both CST Microwave Studio and HFSS Software The antenna array prototype has been built and carried out. The proposed smart structure provides a bandwidth of 480 MHz around operating frequency of 3 GHz with a total gain of about 6 dBi.

Keywords— Antenna array, Compact, CST microwave studio, Early breast cancer detection, Radiometry, Flexible, HFSS software.

I. INTRODUCTION

Breast cancer is a significant health issue affects one in every seven women [1], [2]. Early diagnosis and treatment are the hot keys to survive from breast cancer. Various technologies have been implemented to measure a multitude of physical quantities for diagnosis of abnormal medical conditions as well as to provide guidance during therapeutic intervention [3]. However, whether we face advanced imaging systems or simple fixed point measuring devices, performance is fundamentally linked to instrumentation repeatability and reproducibility of the physiological variable under investigation. The quality of medical imaging methods is influenced by several factors the most important being object contrast, blur, noise, artifacts, and distortion [4]. Image blurring due to patient motion is a well known problem in medical modalities such as X-ray imaging, computer tomography (CT), magnetic resonance imaging (MRI), positron emission tomography (PET), single-photon emission computed tomography (SPECT), and ultrasound imaging [4],

This work was supported by projects NATO (CBP.NUKR.SFP984173) and European Communities Seventh Framework Programs: SEA-on-a-CHIP (FP7-OCEAN-2013) No.614168, and funding from the European Union's Horizon 2020 research and innovation program entitled HEARTEN, No 643694.

A. Afyf and L. Bellarbi are with Higher National School of Technical Education (ENSET)/ Rabat/ Morocco.(corresponding author Email: afyf.amal@gmail.com)

F.Riouch is with National Institute of Post and Telecommunications (INPT)/ Rabat/ Morocco.

A. Errachid is with Institute of Analytic Sciences (ISA) Lyon University /France.

M.A. Sennouni is with LITEN Laboratory of FST-Settat,university Hassan the first /Morocco.

[5]. Motion blurring typically occurs if the patient moves during image acquisition. Unfortunately, involuntary and

uncontrollable motion of internal organs (e.g., respiratory movement) is also a contributing factor. Passive methods like microwave radiometry [6]–[9] and infrared (IR) thermography [10]–[12] are sensing techniques that can read noninvasive temperatures of superficial tissue. For these methods, the emitted power from an object is spontaneous thermal radiation in the microwave or infrared frequency bands. Infrared thermography is used in breast cancer detection [13], [14], imaging of varicose and subcutaneous veins [15], vein pattern biometric [16], and inflammatory detection [17], to mention a few. Complementary microwave radiometry, with less spatial resolution but significantly higher sensing depth than IR thermography, has been investigated for brain temperature monitoring in infants [18], hyperthermia temperature monitoring [19], and breast cancer detection [20]–[22]. A recently proposed application for radiometry is detection of vesicoureteral reflux (VUR) in relatively young patients (<4 years) [23]–[26]. VUR is a condition in which bladder urine flows back through the ureters and into the kidneys [27].

A. Motivation to use Microwave Radiometry in Medicine

Microwave radiometry has explicit low investment costs and low technological complexity, also low spatial resolution compared to the other modalities as seen in table 1.

Table 1. Comparison of some imaging methods.

Modality	Cost	Hardware complexity	Resolution
X-ray	Moderate	Moderate	High
PET	High	High	High
Gamma camera	Moderate	Moderate/High	Moderate
MRI	High	High	High
Ultrasound	Moderate	Moderate	Moderate
IR	Moderate	Moderate/High	High
Radiometry	Low	Low	Low

Other advantages of this method are that it can see at depth of the human body and instrumentation and applicator can be made practically small.

B. Principle of Radiometers

A microwave radiometer is a sensitive instrument that can read temperatures noninvasively in a human body [6], [28] – [31]. The instrument measures the naturally radiated noise power that is emitted from all sources above absolute zero when the material is lossy. Blackbody spectral radiance B at temperature T at any given frequency is given by Planck’s law. For frequencies in the microwave region and temperatures relevant in microwave radiometry, Planck’s law can be approximated by Rayleigh–Jean’s law [32]

$$B(f, T) = \frac{2KTf^2}{c^2} \tag{1}$$

from which, the tissue temperature T (in K) can be written as [1], [33]

$$T = \frac{P}{K \times \Delta F} \tag{2}$$

where ΔF is the antenna bandwidth in MHz, K is Boltzmann’s constant, and P is the power available at the antenna port. The temperature read during this experiment is given by the radiometric equation [34]

$$T_B = (1 - \rho) \int_V W(r) T(r) dV + (1 - \rho) T_{ext} + T_{sys} \tag{3}$$

where T_B is the brightness temperature of the object, ρ is the power reflection coefficient, $W(r)$ is the radiometric weighting function, $T(r)$ is the spatial temperature of the object at the position r , T_{ext} is the electromagnetic interference and T_{sys} the equivalent noise temperature in the radiometer system. The radiometric weighting function is given by

$$W(r) = \frac{\sigma_m(r) |E(r)|^2}{\int_V \sigma_m(r) |E(r)|^2 dV} \tag{4}$$

where E is the electric field intensity of a lossy medium and σ_m is the medium conductivity for a specific frequency with all terms of loss included. The radiometric weighting function is normalized according to [32], [35].

$$\int_V W(r) dV \equiv 1 \tag{5}$$

The technique can be used to form an image with low resolution. An example is given in Fig.1. where 9 probe responses from a breast are used to form the image Fig.2.

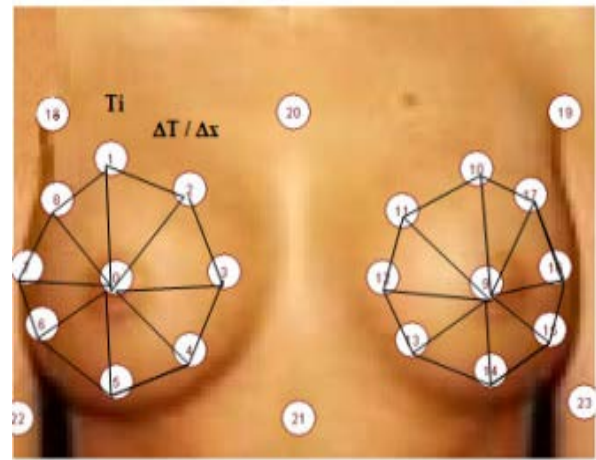


Fig.1 Schematic representation of the measurement points

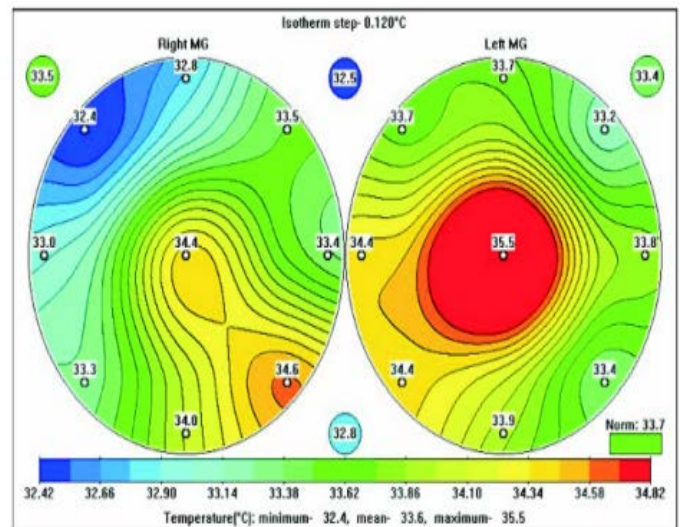


Fig.2 Example of a microwave radiometry image of human breast. The left is a healthy breast and right is a breast with cancer [36].

C. Flexible antennas for Radiometers

Recent years have witnessed a great deal of interest from both academia and industry in the field of flexible electronics. In fact, this study tops the pyramid of research priorities requested by many national research agencies. According to market analysis, the revenue of flexible electronics is estimated to be 30 billion USD in 2017 and over 300 billion USD in 2028 [37]. Their light weight, low-cost manufacturing, ease of fabrication, and the availability of inexpensive flexible substrates (i.e.: papers, textiles, and plastics) make flexible electronics an appealing candidate for the next generation of consumer electronics [38]. Moreover, recent developments in miniaturized and flexible energy storage and self-powered wireless components paved the road for the commercialization of such systems [39]. Consistently, flexible antennas operating in specific frequency bands to provide wireless connectivity are highly demanded by today’s information oriented society, where antennas are the most crucial components in a microwave radiometer as shown in Fig. 3.

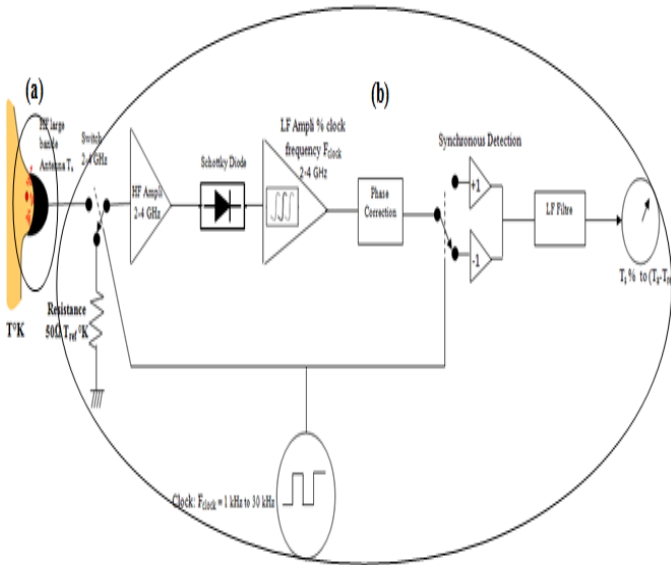


Fig.3 Microwave radiometry system, (a) Antenna array, and (b) Synchronous Detection.

Based on the above references, we propose a flexible antenna array with two elements, having I-shaped slots and a tuning stub which is designed as an RF receiver. This paper is organized as followed: Section II and III respectively introduce, Design Procedures and Simulation Results for both elementary and antenna array. Conclusion is shown in Section IV. As described in subsequent sections, the optimization of antenna structures was carried out by simulations with CST Microwave Studio [40], and Ansoft HFSS [41].

II. ELEMENTARY ANTENNA

A. Antenna Design

The elementary antenna is a thin rectangular patch printed on a Kapton Polyimide substrate having a thickness of $HS=0.125\text{mm}$. The antenna design required to look into the permittivity or dielectric constant of the substrate, width, length of the patch antenna and the ground plane. The permittivity of the substrate plays a major role in the overall performance of the antenna. It affects the width, the characteristic impedance, the length and therefore the resonant frequency that resulting to reduce the transmission efficiency. Using a permittivity value ϵ_r of 3.4, the effective dielectric constant ϵ_{reff} of the antenna is determined from the (6) which was obtained from [42].

$$\epsilon_{\text{reff}} = \frac{\epsilon_r + 1}{2} + \frac{\epsilon_r - 1}{2} \left[1 + 12 \frac{h}{w} \right]^{-1/2} \quad (6)$$

In the xy-plane due to fringing effects, the dimensions of patch along its length is extended by a distance ΔL , which is a function of the effective dielectric constant ϵ_{reff} and the width-to-height ratio (W/h). In addition the length L of the patch determines the resonant frequency and is calculated using (2) and (3)

$$L = \frac{\lambda}{2} - \Delta L = \frac{1}{2f_r \sqrt{\epsilon_{\text{reff}}} \sqrt{\mu_0 \epsilon_0}} - 2\Delta L \quad (7)$$

$$\Delta L = 0.412 \times h \times \left(\frac{\epsilon_{\text{reff}} + 0.3}{\epsilon_{\text{reff}} - 0.258} \right) \left(\frac{\frac{w}{h} + 0.264}{\frac{w}{h} + 0.8} \right) \quad (8)$$

The width W of the patch is critical in terms of power efficiency, antenna impedance and bandwidth. It is dependent on the operating frequency and the substrate dielectric constant.

Equation (4) was used to determine the width.

$$W = \frac{1}{2f_r \sqrt{\mu_0 \epsilon_0}} \sqrt{\frac{2}{\epsilon_r + 1}} = \frac{v_0}{2f_r} \sqrt{\frac{2}{\epsilon_r + 1}} \quad (9)$$

To preserve the flexibility of the antenna, the rectangular radiator with two symmetrical I-slots is fed by a coplanar waveguide transmission line ensuring 100Ω characteristic impedance. The two conducting vias also pass through the dielectric substrate as shown in fig.4.

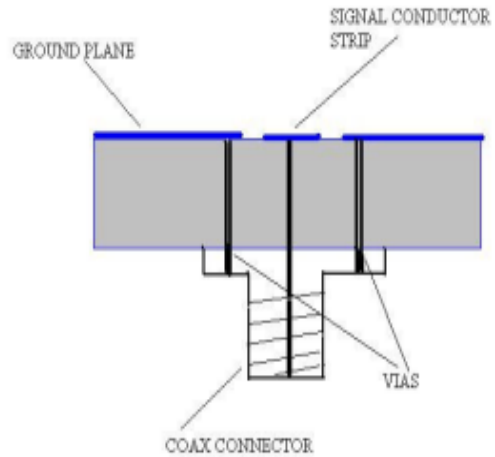


Fig. 4. A schematic diagram of coaxial [43].

Hence the main goal is to develop a receiving antenna with good performances working in S-band at 3 GHz which can provides a good penetration into the breast tissue. Then to achieve the goal, several optimisation processes were applied by using an optimization solver in CST Microwave Studio. Fig.5 presents the geometry shape of the proposed design with parameters shown before. Also Table 2. below presents the various optimized parameters of the proposed elementary antenna.

TABLE 2. PHYSICAL DIMENSIONS OF THE ELEMENTARY ANTENNA

Parameters	Values (mm)	Parameters	Values (mm)
W	15	L _S	9
L	20	W _S	0.5
W _A	14	H _S	0.125
L _A	12	T _M	0.035
L _G	5	G	0.25
W _F	3.122	L _F	7

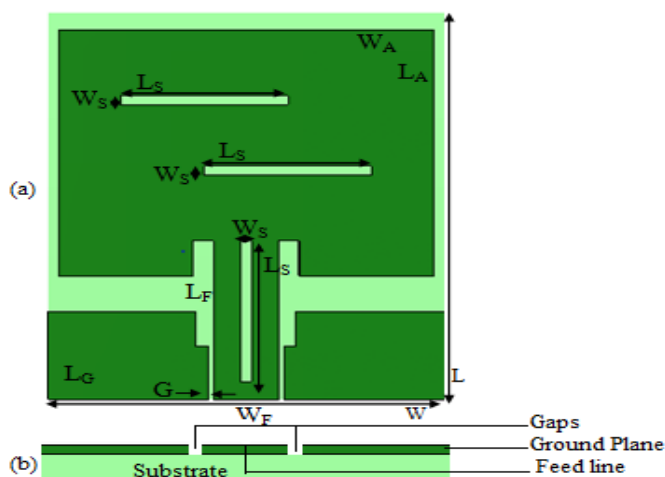


Fig. 5. Elementary flexible CPW antenna, (a) Front view, (b) Bottom view.

B. Simulation Results

It's reported in literature that abnormal both tissues and it surrounding area are warmer than normal's [44], which mean a self radiation with a weak power. This report overviews the design and optimization of a novel microwave receiver antenna which must serves as an element in a radiometric system for early breast cancer detection.

According to Nyquist low (2) and for getting the emitted difference of temperature generated by a tissue located at a depth of about 3cm, the microwave radiometer can indicate a previous anomaly at operating frequency around 3GHz [45]. As shown in Fig. 6, the return loss of the elementary antenna is about -22.58dB with a large bandwidth of 480 MHz at center frequency of 3.09 GHz, which means a good matching input impedance is achieved at the operating frequency, also Fig. 7 depicts the VSWR obtained for 3GHz, that is 1.16 (less than 2), within the recommended range. Thus, the simulation results indicate that the antenna is well matched at 3.09GHz and a maximum possible amount of energy is absorbed at the input terminal with a minimum reflected power.

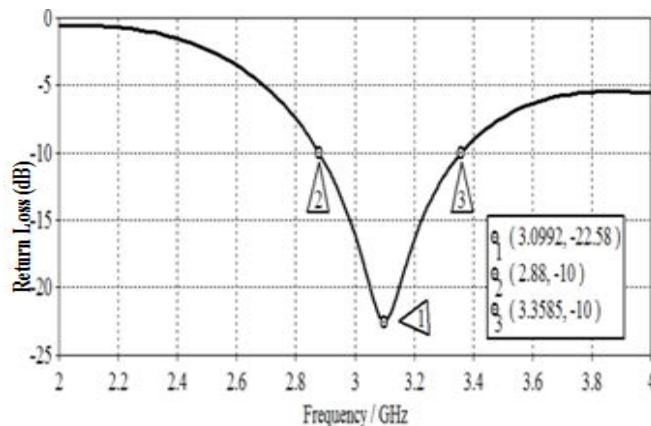


Fig.6. Simulated Return Loss of the elementary antenna

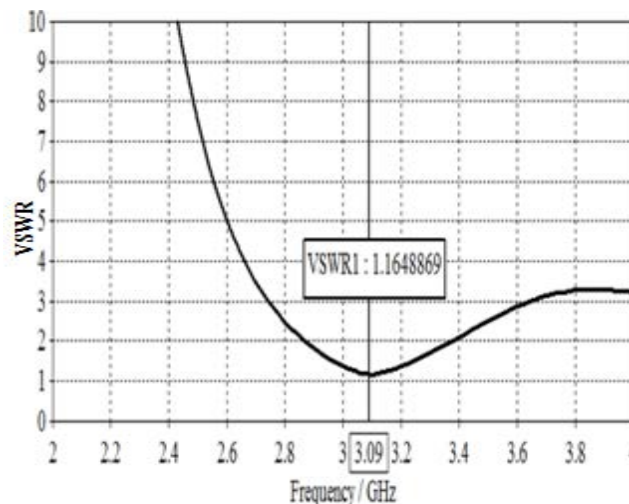


Fig.7. Simulated VSWR of the elementary antenna

Fig.8 presents the 3D-radiation pattern with the structure below at 3.1GHz. Further Fig.9 represents the gain versus frequency that is almost around 3 GHz with a peak gain of about 1dB which is not sufficient for microwave thermography using microwave radiometry.

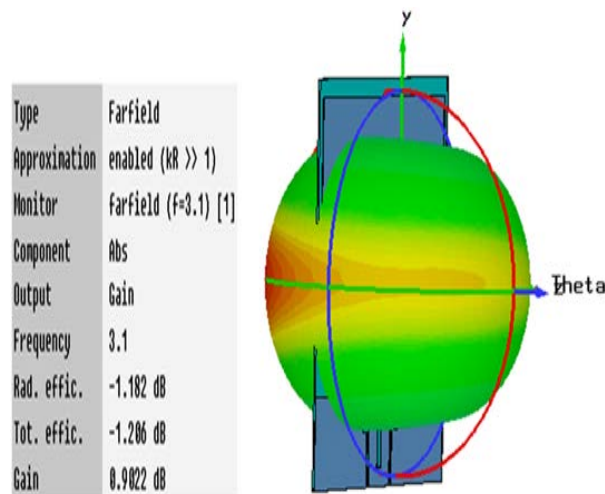


Fig.8. 3D radiation pattern @3GHz

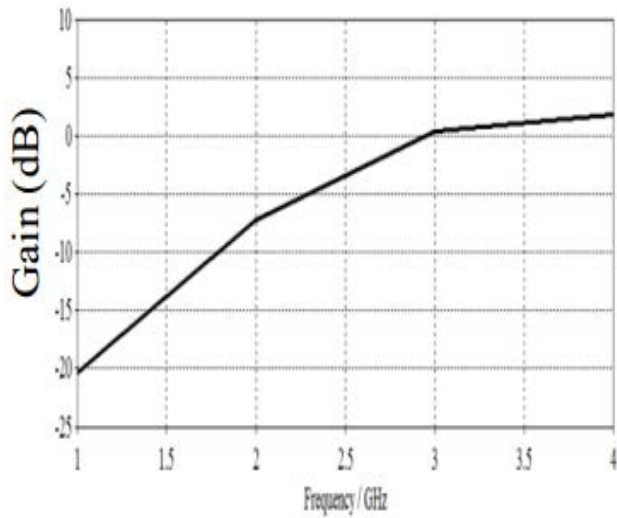


Fig.9. Antenna gain versus frequency of the elementary antenna

Fig. 10 presents a comparison between the proposed antenna and some recently developed miniaturized flexible antennas. Compared with the other structures the proposed antenna shows a wide impedance bandwidth around the operating frequency, compact size, and an important gain.

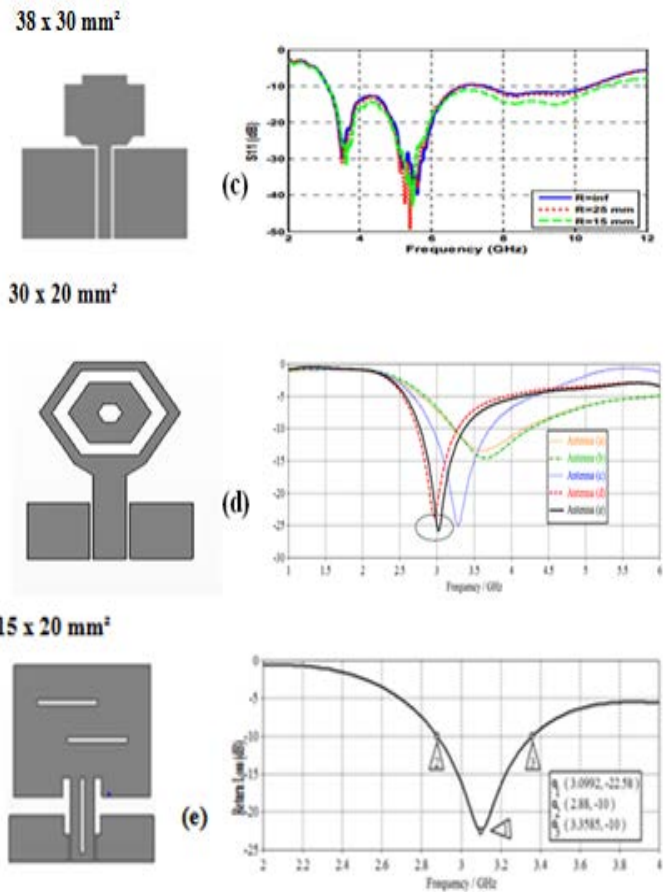
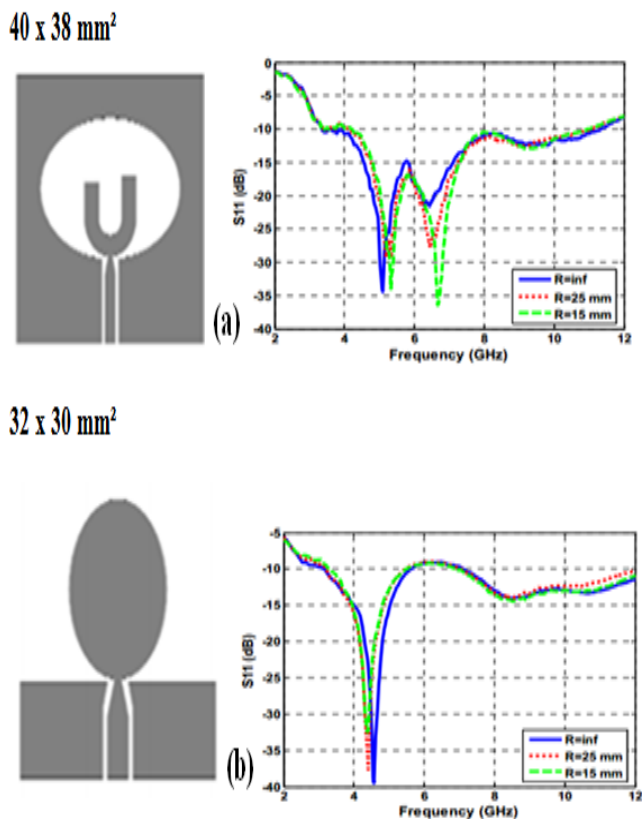


Fig.10. (a), (b), (c) , and (d) respectively from [24], [25], [26], and [2], (e) Our proposed antenna.

III. ANTENNA ARRAY

A. Design process

In order to increase the antenna gain and directivity by preserving the operating frequency in S-band at 3 GHz, we have started from the elementary antenna optimized before and we have modeled an array of two-Element printed on the top layer of the same substrate used for the elementary antenna presented above, with the arrangement shown in Fig.6. We have chosen this arrangement to minimize the effects of coupling and the generation of higher modes, also to reduce the array occupation area. A T-power junction has been used to transmit power to the array elements, in addition the CPW feed line with a characteristic impedance of 50 Ω is also used to excite the global antenna array. Further a tuning stub with an optimized dimensions and position is added to the CPW feed to improve the antenna array performances. The proposed antenna array has an overall size of about 5.3cm x5cm with the geometry along with the parameters of the antenna array which are shown in Fig.11.(c).

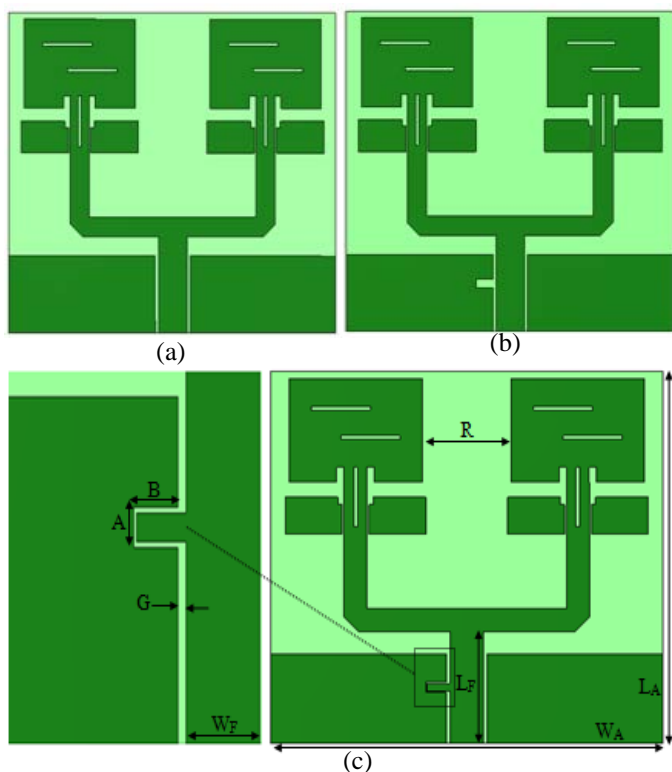


Fig.11. Proposed antenna array (a) with simple ground, (b) with shaped ground, and (c) with a tuning stub. ($G=0.15\text{mm}$, $W_A=53\text{mm}$, $L_A=50\text{mm}$, $R=10\text{mm}$, $W_F \times L_F=4.8\text{mm} \times 12.5\text{mm}$, $A \times B=2\text{mm} \times 4\text{mm}$)

B. Simulation Results and Discussion

To show the effect of the tuning stub, a comparative study has been applied. It is seen that the tuning stub can shift the operating frequency from 3.4 GHz to 3 GHz providing a good impedance matching for the antenna array with a return loss of about -35 dB at the operating frequency of 3GHz and an important bandwidth of 480MHz which is from 2.72 GHz to 3.2 GHz. Fig. 12 shows the simulated return loss of the proposed design.

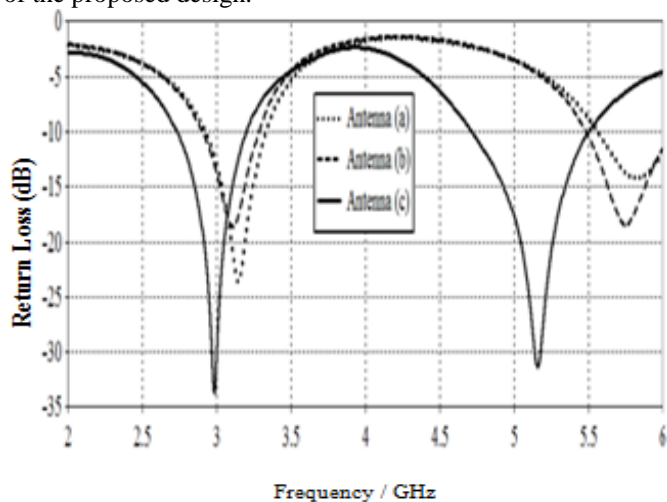


Fig.12 Return Loss vs. Frequency for the three antenna structures: (a), (b), and (c)

We have applied another method to prove the antenna array results by using the FEM (Finite Element Method) introduced by HFSS software. Fig.13 and Fig.14 shows the comparison results with the two methods. The results show that the proposed antenna array is operating at the same frequency range (S -band, 2-4GHz) for both software with a good input matching and approximately the same bandwidth.

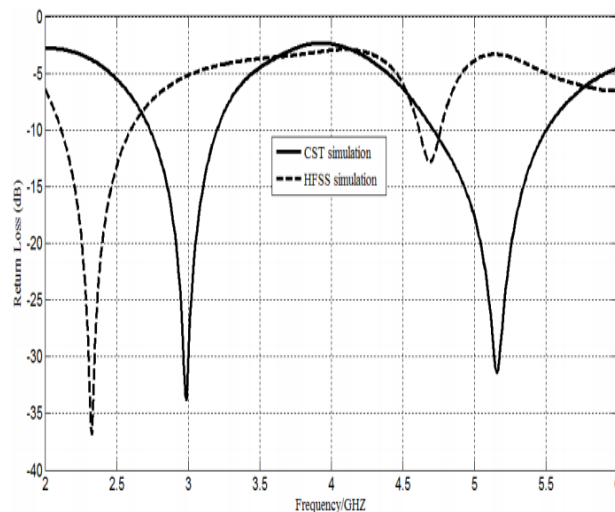


Fig.13 The return loss of the proposed antenna array with CST&HFSS

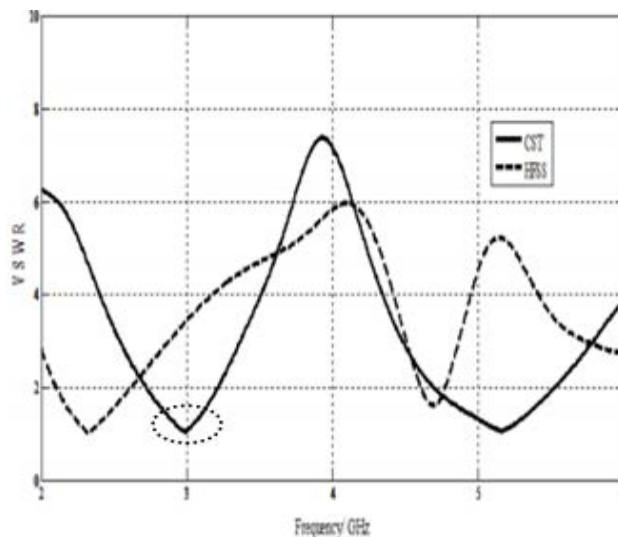


Fig.14 VSWR of the proposed antenna array with CST&HFSS

The radiation pattern taken for the far-field at 3GHz is indicated in Fig.15 and Fig.16. Results indicates that the antenna array provides a directional behavior in E-plan (for $\text{PHY}=0^\circ$) and omnidirectional's behavior in H-plan (for $\text{THETA}=0^\circ$). Furthermore Fig.16 presents the normalized gain against frequency of the developed antenna array. The results show that the design provides an important gain that is almost around 5 dB in the frequency range below 2.7 GHz. However at the operating frequency of 3 GHz the design exhibits a gain of about 5.3 dB which is perfectly sufficient and suitable for microwave thermography.

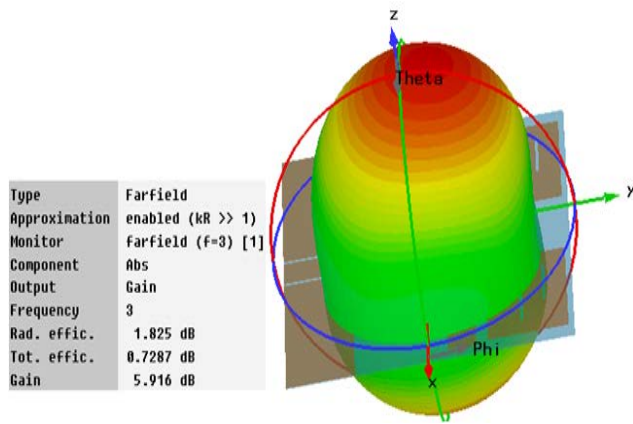


Fig.15 3D radiation pattern for the antennas array @ 3GHz

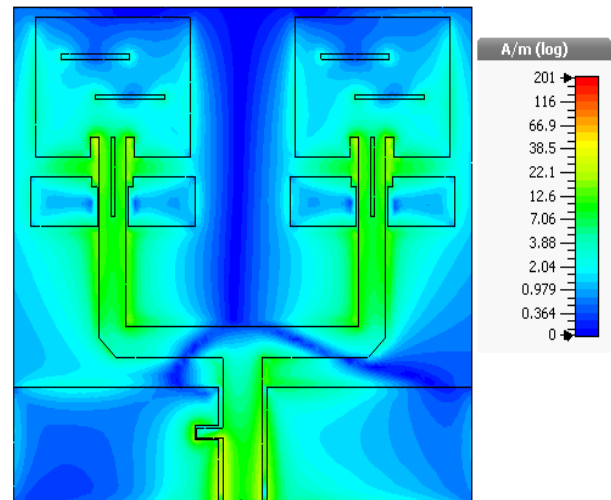


Fig.18 Simulated surface currents at 3GHz of antenna array

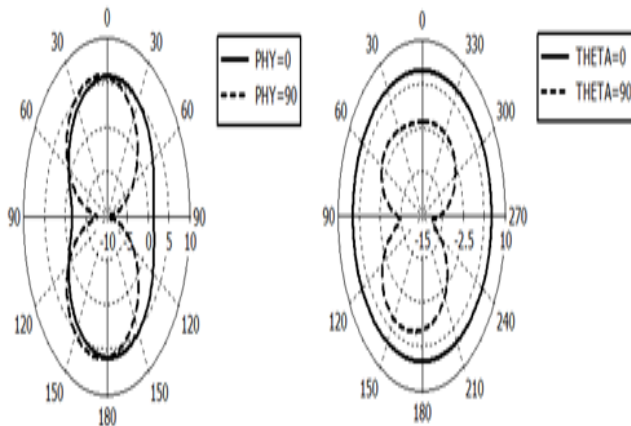


Fig.16 2D polar radiation pattern @ 3GHz for the antenna array; (a) E-Plan, and (b) H-Plan.

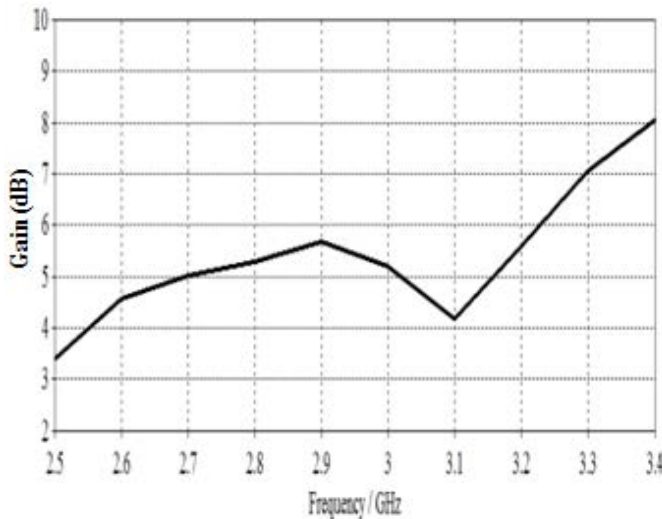


Fig.17 Antenna gain versus frequency

Current distribution determines how the current flows on the patch of the antenna array. Fig. 18 demonstrates these results at 3 GHz. We observe a high strength of current radiates along the transmission lines, at the tuning stub and in the edges of the array patches.

IV. CONCLUSION

A novel CPW microstrip antenna array has been successfully designed and simulated using CST Microwave Studio and HFSS Software. The performance criteria extracted from the software includes return loss, VSWR, radiation pattern, and surface currents provide clear indication that the proposed design, has the required performances to be investigated in a microwave radiometry system as well as for wearable applications, due to its miniature size (5.3cm x5 cm), low profile and weight and very thin substrate. Also the important gain (6dBi) and the large bandwidth (480MHz around the center frequency of 3 GHz), provided by the developed antenna; are good features to improve the radiometer sensitivity at very low power densities transmitted by the self-radiation of abnormal breast tissue. Future work will focus to validate the simulated results of the developed antenna array by measurements and associate it with a synchronous detector to complete the microwave radiometer system.

ACKNOWLEDGMENT

The authors would like to thank the contribution of the professor Abdelhamid Errachid from Institute of Analytic Sciences (ISA) of Lyon University in France and all members of LGE laboratory of ENSET/ENSIAS, Rabat in Morocco for their technical and financial support in this research.

REFERENCES

[1] A.Afyf And L.Bellarbi, A. Errachid, M. A. Sennouni, "Flexible Microstrip CPW Slated Antenna for Breast Cancer Detection", 1 st International Conference on Electrical and Information Technologies, 2015.

[2] A.Afyf and L.Bellarbi, F. Riouch, A. Achour, A. Errachid, M. A. Sennouni, "Flexible Miniaturized UWB CPW II- shaped Slot Antenna for Wireless Body Area Network (WBAN) Applications", Published in the third International Workshop on RFID And Adaptive Wireless Sensor Networks (RAWSN), 2015.

- [3] J. G. Webster, *Medical Instrumentation, Application and Design*, 4th ed. New York: Wiley, 1998.
- [4] J. Perry Sprawls, *Physical Principles of Medical Imaging*. Philadelphia, PA: Lippincott Williams and Wilkins, 1987.
- [5] J. T. Bushberg, J. A. Seibert, and E. M. L., Jr, J. M. Boone, *The Essential Physics of Medical Imaging*, 2nd ed. ed. Philadelphia, PA: Lippincott Williams & Wilkins, 2002.
- [6] S. Mizushima, H. Ohba, K. Abe, S. Mizoshira, and T. Sugiura, "Recent Trends in Medical Microwave Radiometry," *IEICE Trans. Commun.*, vol. E78-B, no. 6, 1995.
- [7] B. Stec, A. Dobrowolski, and W. Susek, "Multifrequency microwave thermograph for biomedical applications," *J. Telecommun. Inf. Technol.*, pp. 117–122, 2004.
- [8] S. Mizushima, T. Shimuzu, K. Suzuki, M. Kinomura, H. Ohba, and T. Sugiura, "Retrieval of temperature-depth profiles in biological objects from multi-frequency microwave radiometric data," *J. Electromagn. Waves App.*, vol. 7, no. 11, pp. 1515–1548, 1993.
- [9] Y. Leroy, "Microwave radiometry and thermography. present and prospective," *Biomed. Thermol.*, pp. 485–499, 1982.
- [10] S. Bagavathiappan, T. Saravanan, J. Philip, T. Jayakumar, B. Raj, R. Karunanithi, T. Panicker, M. P. Korath, and K. Jagadeesan, "Infrared thermal imaging for detection of peripheral vascular disorders," *J. Med. Phys.*, vol. 34, pp. 43–47, 2009.
- [11] B. Jones and P. Plassmann, "Digital infrared thermal imaging of human skin," *IEEE Eng. Med. Biol.*, vol. 21, no. 6, pp. 41–48, Nov./Dec. 2002.
- [12] B. F. Jones, "A reappraisal of the use of infrared thermal image analysis in medicine," *IEEE Trans. Med. Imag.*, vol. 17, no. 6, pp. 1019–1027, Dec. 1998.
- [13] J. Head and R. Elliott, "Infrared imaging: making progress in fulfilling its medical promise," *IEEE Eng. Med. Biol. Mag.*, vol. 21, no. 6, pp. 80–85, Nov./Dec. 2002.
- [14] N. A. Diakides and J. D. Bronzino, *Medical Infrared Imaging*. Boca Raton, FL: CRC Press. Taylor & Francis Group, 2008.
- [15] V. P. Zharov, S. Ferguson, J. F. Eidt, P. C. Howard, L. M. Fink, and M. Waner. (2004). "Infrared imaging of subcutaneous veins". *Lasers Surg. Med.* 34(1), pp. 56–61, [Online]. Available: <http://dx.doi.org/10.1002/lsm.10248>
- [16] L. Wang and G. Leedham, "Near- and far-infrared imaging for vein pattern biometrics," in *Proc. Adv. Video Signal Based Surveill.*, IEEE Conf., 2006, p. 52.
- [17] T.C. Chang, Y.L. Hsiao, and S.L. Liao. (2008). "Application of digital infrared thermal imaging in determining inflammatory state and follow-up effect of methylprednisolone pulse therapy in patients with graves ophthalmopathy". *Graefe's Arch. Clin. Exp. Ophthalmol.* [Online]. 246, pp.45–49, 10.1007/s00417-007-0643-0. Available: <http://dx.doi.org/10.1007/s00417-007-0643-0>
- [18] K. Maruyama, S. Mizushima, T. Sugiura, G. V. Leeuwen, J. Hand, G. Marrocco, F. Bardati, A. Edwards, D. Azzopardi, and D. Land, "Feasibility of noninvasive measurement of deep brain temperature in newborn infants by multifrequency microwave radiometry," *IEEE Trans. Microw. Theory Tech.*, vol. 48, no. 11, pp. 2141–2147, Nov. 2000.
- [19] K. Arunachalam, P. R. Stauffer, P. F. Maccarini, S. Jacobsen, and F. Sterzer, "Characterization of a digital microwave radiometry system for noninvasive thermometry using a temperature-controlled homogeneous test load," *Phys. Med. Biol.*, vol. 53, no. 14, 2008.
- [20] F. Bardati and S. Iudicello, "Modeling the visibility of breast malignancy by a microwave radiometer," *IEEE Trans. Biomed. Eng.*, vol. 55, no. 1, pp. 214–221, Jan. 2008.
- [21] B. Bocquet, J. C. V. Velde, A. Mamouni, Y. Leroy, G. Giaux, J. Delannoy, and D. Delvallee, "Microwave radiometric imaging at 3 ghz for the exploration of breast tumors," *IEEE Trans. Microw. Theory Tech.*, vol. 38, no. 6, pp. 791–793, Jun. 1990.
- [22] R. Tipa and O. Baltag, "Microwave thermography for cancer detection," presented at the 5th International Balkan Workshop on Applied Physics, Constanta, Romania., 2004.
- [23] B. W. Snow and M. B. Taylor. (2010). Non-invasive vesicoureteral reflux imaging. *J. Pediatr. Urol.* [Online]. 6(6), pp. 543–549. Available: doi:10.1016/j.jpuro.2010.02.211
- [24] B. Snow, K. Arunachalam, V. D. Luca, P. Maccarini, Ø. Klemetsen, Y. Birkelund, T. J. Pysker, and P. Stauffer. (2011). "Noninvasive vesicoureteral reflux detection: Heating risk studies for a new device". *J. Pediatr. Urol.*, to be published, [Online]. Available: <http://www.sciencedirect.com/science/article/pii/S1477513111001331>
- [25] K. Arunachalam, P. F. Maccarini, V. De Luca, F. Bardati, B. W. Snow, and P. R. Stauffer, "Modeling the detectability of vesicoureteral reflux using microwave radiometry," *Phys. Med. Biol.*, vol. 55, no. 18, p. 5417, 2010.
- [26] K. Arunachalam, P. Maccarini, V. De Luca, P. Tognolatti, F. Bardati, B. Snow, and P. Stauffer, "Detection of vesicoureteral reflux using microwave radiometry - system characterization with tissue phantoms," *IEEE Trans. Biomed. Eng.*, vol. 58, no. 6, pp. 1629–1636, Jun. 2011.
- [27] A. Guyton and J. Hall, *Textbook of Medical Physiology*, 10th ed. ed. Philadelphia, PA: W.B. Saunders Company, 2000.
- [28] K. L. Carr, "Microwave radiometry: Its importance to the detection of cancer," *IEEE Trans. Microw. Theory Tech.*, vol. 37, no. 12, pp. 1862–1869, Dec. 1989.
- [29] D. Land, "Radiometer Receivers for Microwave Thermography," *Microw. J.*, pp. 196–201, May 1983.
- [30] Y. Leroy, A. Mamouni, J. V. D. Velde, B. Bocquet, and B. Dujardin, "Microwave radiometry for non-invasive thermometry," *Automedica*, vol. 8, pp. 181–202, 1987.
- [31] Y. Leroy, B. Bocquet, and A. Mamouni, "Non-invasive microwave radiometry thermometry," *Physiol. Meas.*, vol. 19, pp. 127–148, 1998.
- [32] R. Reeves, A. Anson, and D. Landen, *Manual of Remote Sensing*, vol. I, 1st ed. ed. Falls Church, VA: American Society of Photogrammetry, 1975.
- [33] F. Ulaby, R. Moore, and A. Fung, "Microwave remote sensing fundamentals radiometry," in *Microwave Remote Sensing*, vol. I, 1st ed. ed. Norwood, MA: Artec House, 1981.
- [34] S. Jacobsen and Ø. Klemetsen, "Improved detectability in medical microwave radio-thermometers as obtained by active antennas," *IEEE Trans. Biomed. Eng.*, vol. 55, no. 12, pp. 2778–2785, Dec. 2008.
- [35] S. Jacobsen and P. Stauffer, "Multifrequency radiometric determination of temperature profiles in a lossy homogeneous phantom using a dual-mode antenna with integral water bolus," *IEEE Trans. Microw. Theory tec.*, vol. 50, no. 7, pp. 1737–1746, 2002.
- [36] M. Costin, O. Baltag, C. Ștefănescu, A. Ciobanu, and S. Bejinariu, "Microwave Medical Imaging in a Non-Invasive Breast Cancer Diagnosis System", 7th WSEAS International Conference on Applied Computer Science, Venice, Italy, November 21-23, 2007.
- [37] J. Hu, "Overview of flexible electronics from ITRIs viewpoint". *VLSI Test Symposium (VTS)*, 2010 28th, 19-22 April, 84.
- [38] A. Nathan, B. Chalamala, "Special Issue on Flexible Electronics Technology, Part 1: Systems and Applications". *Proceedings of the IEEE*, 93(7), 1235-1238, 2005.
- [39] Y. Huang, C. Jiankui, Y. Zhouping, X. Youlun, "Roll-to-Roll Processing of Flexible". 2014.
- [40] CST Microwave Studio Suite 2011, www.cst.com.
- [41] Ansoft HFSS Software, <http://www.ansys.com>.
- [42] R. Karli, H. Ammor, J. Elaoufi, "Miniaturized UWB Microstrip Antenna for Microwave Imaging". *WSEAS transactions on information science and applications*, 2014.
- [43] J. Nithianandam, "A Wide-Band CPW Patch-Slot Antenna for Telemetry Applications". *Proc. of the 8th WSEAS Int. Conf. on data networks, communications, computers*. 2009.
- [44] H. Ellis, G. Colborn., J.E. Skandalakis, "Surgical embryology and anatomy of breast and its related anatomic structures, *Surgical Clinic*", North America, vol. 73, 1993, pp. 611-32.
- [45] C.E. Jacobi, B. Siegerink, C.J. Asperen. (2009). "Differences and similarities in breast cancer risk assessment models in clinical practice: which model to choose?", *Breast Cancer Res Treat*, 115: 381–90.